566 *Biochemistry* **2011,** *50,* 566–573
DOI: 10.1021/bi101639y

BIOCHEMISTRY
including biophysical chemistry & molecular biology
Article

Molecular and Structural Insight into the Role of Key Residues of Thrombospondin-1 and Calreticulin in Thrombospondin-1−Calreticulin Binding[†]

Qi Yan,[‡] Joanne E. Murphy-Ullrich,[§] and Yuhua Song*[,‡]

[‡]*Department of Biomedical Engineering and* [§]*Department of Pathology, The University of Alabama at Birmingham, Birmingham, Alabama 35294, United States*

Received October 12, 2010; Revised Manuscript Received December 13, 2010

ABSTRACT: Thrombospondin-1 (TSP1) binding to calreticulin (CRT) on the cell surface signals focal adhesion disassembly, leading to the intermediate adhesive phenotype, cell migration, anoikis resistance, and collagen stimulation. Residues Lys 24 and 32 in TSP1 and amino acids 24−26 and 32−34 in CRT have been shown through biochemical and cell-based approaches to be critical for TSP1−CRT binding and signaling. This study investigated the molecular and structural basis for these key TSP1 and CRT residues in TSP1−CRT binding. On the basis of a validated TSP1−CRT complex structure, we adopted steered molecular dynamics simulations to determine the effect of mutation of these key residues on TSP1−CRT binding and validated the simulation results with experimental observations. We further performed 30 ns molecular dynamics simulations for wild-type TSP1, CRT, K24A/K32A mutant TSP1, and mutant CRT (residues 24−26 and 32−34 mutated to Ala) and studied the conformational and structural changes in TSP1 and CRT as the result of mutation of these critical residues. Results showed that mutation of residues 24 and 32 to Ala in TSP1 and of amino acids 24−26 and 32−34 to Ala in CRT results in a shortened β-strand in the binding site, decreased hydrogen bond occupancy for β-strand pairs that are located within or near the binding site, increased conformational flexibility of the binding site, a changed degree of dynamically correlated motion between the residues in the binding site and the other residues in protein, and a changed degree of overall correlated motion between the residues in the protein. These changes could directly contribute to the loss or weakened binding between TSP1 and CRT and the resultant effects on TSP1−CRT binding-induced cellular activities. Results from this study provide a molecular and structural insight into the role of these critical residues of TSP1 and CRT in TSP1−CRT binding.

Cell adhesion between cells and the extracellular matrix is a multistep process that is initiated by the binding of a ligand in the extracellular matrix to a cell surface receptor, triggering cell spreading and the formation of focal adhesions and stress fibers (*1*). Cell−matrix adhesion is also a reversible process in which a cell moves from a state of stronger adherence to a state of weaker adherence (*1*, *2*). Intermediate adhesion is an adaptive condition and is characterized by a restructuring of focal adhesions and stress fibers during the maintenance of a spread cell shape, i.e., focal adhesion disassembly (*1*). Thrombospondin-1 (TSP1)[1] is a protein in the extracellular matrix and in soluble form that interacts with the cell surface protein calreticulin (CRT) to signal intermediate adhesion and regulate cell migration, anoikis resistance, and collagen synthesis (*3*−*9*). TSP1 is a multifunctional matricellular protein that does not directly provide structure to the extracellular matrix but interacts with cells and modifies cellular functions (*10*, *11*). It is a large (420 kDa) disulfide-linked homotrimeric glycoprotein, in which each monomer of TSP1 is composed of N- and C-terminal globular domains connected by a rodlike segment (*12*). CRT, a ubiquitous calcium-binding protein, is composed of a globular β-sandwich N-domain, a proline-rich β-hairpin P-domain, and a calcium-binding C-domain (*13*). The conformation of the CRT P-domain shows a spiral-like shape and indicates conformational flexibility of the CRT P-domain (*14*, *15*). The N-terminal domain of TSP1 binds to the N-domain of CRT to enhance binding of CRT to the LDL receptor-related protein complex (LRP1), signaling intermediate adhesion, cell migration, anoikis resistance, and collagen synthesis in endothelial cells and fibroblasts (*3*−*9*). The CRT binding site in TSP1 has been localized to amino acids 17−35 (ELTGAARKGSGRRLVKGPD), and its functions can be mimicked by a peptide of this sequence, the hep I peptide (*16*). Two lysine residues in the hep I peptide (residues 24 and 32 of the TSP1 N-domain) are critical for the hep I peptide binding to CRT (*3*, *16*). The CRT binding site for TSP1 is an 18-residue sequence (CRT19.36, RWIESKHKSDFGKFVLSS) in the N-terminal domain of CRT (*4*). Two clusters of basic amino acids 24−26 and amino acids 32−34 in this sequence of CRT are critical for TSP1 binding and function (*7*). The crystal structure of the TSP1 N-domain has been determined (*17*). A validated three-dimensional structural model of CRT with the N-domain, P-domain, and partial C-domain has been

[†]This work was supported by TeraGrid supercomputer allocation (National Science Foundation Grant MCB090009) to Y.S. and National Institutes of Health Grant HL79644 to J.E.M.-U.

*To whom correspondence should be addressed: Department of Biomedical Engineering, The University of Alabama at Birmingham, 803 Shelby Interdisciplinary Biomedical Research Building, 1825 University Blvd., Birmingham, AL 35294. Phone: (205) 996-6939. Fax: (205) 975-4919. E-mail: yhsong@uab.edu.

[1]Abbreviations: TSP1, thrombospondin-1; CRT, calreticulin; LRP1, low-density lipoprotein receptor-related protein complex; MD, molecular dynamics; SMD, steered molecular dynamics; rmsd, root-mean-square deviation; rmsf, root-mean-square fluctuation.

 Published on Web 12/13/2010

constructed on the basis of the crystal structure of calnexin and the NMR structure of the P-domain of CRT (*14*, *18*, *19*). A validated complex of the TSP1 N-domain with CRT was constructed (*20*). The structures of the TSP1 N-domain, CRT, and the complex of the TSP1 N-domain and CRT provide a basis for studying the molecular and structural basis for the role of the key residues in TSP1 and CRT in TSP1−CRT binding.

In our recent studies, we investigated the binding thermodynamics of the TSP1−CRT complex and the conformational changes in CRT induced by its binding to TSP1 through combined binding free energy analysis, molecular dynamics simulation, and anisotropic network model restrained molecular dynamics simulation (*20*). We constructed a validated TSP1−CRT complex as shown in Figure 1S of the Supporting Information. We performed binding free energy calculations for the wild-type TSP1−CRT complex, the TSP1 mutant−CRT complex with residues Lys 24 and Lys 32 of TSP1 mutated to Ala (TSP1 K24A/K32A mutant), and the TSP1−CRT mutant complex with residues 24−26 and 32−34 of CRT mutated to Ala, based on the 30 ns MD simulation trajectories. The calculated binding free energies showed that either the K24A and K32A mutations in TSP1 or the mutation of residues 24−26 and 32−34 of CRT to Ala significantly decreased the level of TSP1−CRT binding, which was consistent with previous experimental observations (*3*, *7*, *16*). Analysis of the binding free energy components showed that mutations in TSP1 and CRT resulted in the significant changes in the electrostatic energy, van der Waals energy, polar solvation energy, and entropy of the TSP1−CRT complex, which results from the charge changes in the TSP1−CRT protein complex and the conformational changes in TSP1 and CRT induced by TSP1−CRT interactions. Conformational analyses showed that TSP1 binding to CRT resulted in a more "open" conformation and a significant rotational change for the CRT N-domain with respect to the CRT P-domain, which could expose the potential binding site(s) in CRT for binding to LRP1 to signal focal adhesion disassembly. Although we characterized the effect of the K24A and K32A mutations in TSP1 and the mutation of residues 24−26 and 32−34 of CRT to Ala on TSP1−CRT binding thermodynamics, the effects of these binding site mutations on the structure of TSP1 and CRT and the impact of these structural alterations on TSP1−CRT interactions have not been investigated.

In this study, we simulate the effect of the key residues of TSP1 and CRT on TSP1−CRT binding with steered molecular dynamics simulations, which were consistent with previous biochemical data (*3*, *4*, *7*). We performed 30 ns molecular dynamics (MD) simulations for wild-type TSP1, CRT, TSP1 mutant (residues 23 and 32 mutated to Ala), and mutant CRT (residues 24−26 and 32−34 mutated to Ala) and studied the conformational and structural changes in TSP1 and CRT as a result of mutation of these critical residues. Results from this study provide molecular and structural insight into the role of these critical residues of TSP1 and CRT in TSP1−CRT binding that signals focal adhesion disassembly.

MATERIALS AND METHODS

Steered Molecular Dynamics Simulations. To evaluate the effects of mutations of residues 24 and 32 to Ala in TSP1 and of amino acids 24−26 and 32−34 to Ala in CRT on TSP1−CRT binding, steered molecular dynamics (SMD) simulations with a constant-velocity protocol were used to probe the unbinding procedure of the TSP1−CRT complex, the TSP1 K24A/K32A mutant−CRT complex, and the TSP1−CRT mutant complex. We used the NAMD 2.6 MD package (*21*) for SMD simulations, and the AMBER force field was used for the simulated systems. The validated TSP1−CRT complex obtained from the previous study (*20*) and its mutant were separately solvated with TIP3P water molecules (*22*) and a 150 mM NaCl physiological salt concentration in a periodic box, and 1 nm of solvent between the protein and the box boundaries was ensured to reduce potential artifacts arising from periodicity. Before SMD simulations, we performed energy minimization and equilibration of the water, and the warm-up of the simulated system with a standard protocol similar to that of our previous MD simulation studies (*20*, *23*−*26*). For the system heated to 300 K, we further implement the SMD simulations to probe the effect of mutations of residues 24 and 32 to Ala in TSP1 and of amino acids 24−26 and 32−34 in CRT to Ala on the unbinding of the TSP1−CRT complex. Instead of applying the pulling force only on one point to mimic the atomic force microscopy (AFM) as in previous studies (*27*−*29*), which could break the secondary structure of the protein, we applied the pulling forces at a constant speed of 0.2 Å/ps, which was chosen as a balance of the complex unbinding procedure and proper simulation time scale, on the C_α atom of each residue on β-sheets of TSP1 except the residues in the CRT binding site. The residues in the structurally stable N-domain and the partial C-domain of CRT, except the residues in the binding site for TSP1, were treated as rigid and were fixed and leave the structurally flexible P-domain of CRT as an unfixed and flexible region (Figure 1). The pulling direction was along the center of mass of the pulled residues and the fixed residues. Force

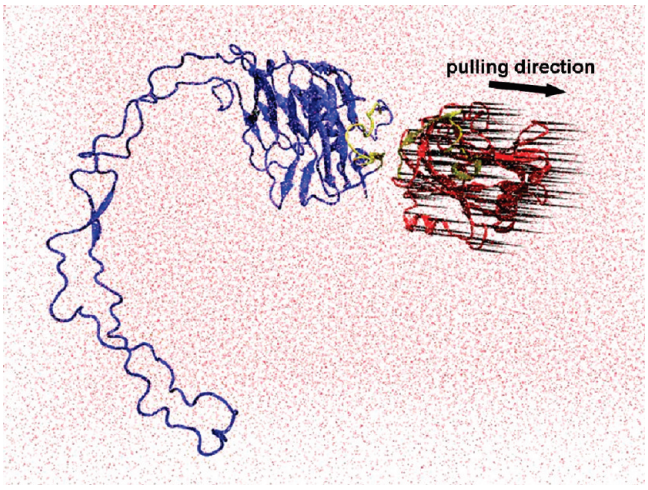

FIGURE 1: Setup of the SMD simulation. The TSP1−CRT complex was solvated in water. Pulling force was applied on the α-carbons over β-sheets of TSP1 except the residues in the binding site for CRT. The residues in the structurally stable N-domain and the partial C-domains of CRT, except the residues in the binding site for TSP1, were treated as rigid bodies and were fixed, and the structurally flexible P-domain of CRT was left as an unfixed and flexible region. The pulling direction was along the center of mass of the pulled residues and the fixed residues. Legend: red for TSP1, blue for CRT, yellow for binding sites [the TSP1 binding site for CRT is localized to amino acids 17−35 (ELTGAARKGSGRRLVKGPD), and the CRT binding site for TSP1 is an 18-residue sequence of CRT19.36 (RWIESKHKSDFGKFVLSS)], and red dots for water. The black "porcupine needles" indicate the direction of pulling force applied on the α-carbons over β-sheets of TSP1. The images were made with VMD.

Table 1: Four Systems for 30 ns MD Simulations

system	TSP1 N-domain	CRT
1	wild-type TSP1	
2	TSP1 K24A/K32A mutant	
3		wild-type CRT
4		CRT mutant with mutations of residues 24−26 and 32−34 to Ala

experienced by the C_α atom of the pulled residues was calculated with eq 1 (*28*):

$$F = K(vt - x) \quad (1)$$

where K is the spring constant, set as 7 kcal mol^{-1} Å^{-2} (*30*), v is the pulling velocity, t is the time, and x is the movement of the pulled C_α atom from its original position. The force extension profiles over time experienced by the TSP1−CRT complex and its mutant were compared to determine the effect of K24A and K32A mutations of TSP1 and the mutation of residues 24−26 and 32−34 to Ala in CRT on the unbinding ability of the TSP1−CRT complex. The calculated result was compared with the experimental data for the validation.

In addition to probing the force extension profile experienced by the TSP1−CRT complex and its mutant with constant velocity SMD simulations, we performed constant force SMD by applying constant force to the TSP1−CRT complex and its mutant to obtain the extension profile over time to determine the change in the extension profile of the TSP1−CRT complex caused by the K24A and K32A mutations of TSP1 and the mutation of residues 24−26 and 32−34 to Ala in CRT. We compared the simulation results with the experimental results of biochemical studies (*3*, *16*) for further validation (available as Supporting Information).

Molecular Dynamics Simulations. We performed 30 ns MD simulations for the wild-type TSP1 N-domain (TSP1), the TSP1 K24A/K32A mutant, wild-type CRT, and the CRT mutant with mutations of residues 24−26 and 32−34 to Ala (Table 1) to assess the conformational and structural changes in the TSP1 N-domain and CRT that resulted from the mutations of residues 24 and 32 to Ala in TSP1 and of amino acids 24−26 and 32−34 in CRT to Ala, thus providing molecular and structural insight into the role of the critical residues in TSP1 and CRT in TSP1−CRT binding. We used the AMBER 9 MD package (*31*) for the MD simulations. The MD simulations were performed in a periodic box (the size of the box depends on the simulated system). One nanometer of solvent between the protein and the box boundaries was ensured to reduce potential artifacts arising from periodicity. The periodic box was filled with TIP3P water molecules (*22*) and 150 mM NaCl (physiological salt concentration). Additional Na^+ or Cl^- ions were added to the system to neutralize the charge of the protein complex. The AMBER force field was used for the simulated systems in combination with a standard MD simulation protocol similar to that of our previous studies (*20*, *23*−*26*). Briefly, the MD simulation protocol included (1) steepest descent minimization for the solvent with the protein and ions restrained but with water mobile, (2) equilibration of water with mobile water molecules but with the protein and ions restrained at a constant number, pressure, and temperature (*NpT*) at 50 K and 1 atm for 20 ps, (3) the warm-up of the system via a series of 10 ps constant number−volume−temperature (*NVT*) MD simulations at 50, 100, 150, 200, 250, and 300 K with SHAKE constraints and 2 fs time steps, and (4) production simulation at *NpT*, 300 K, and 1 atm for the assigned time length of 30 ns in this study. In the production simulations, SHAKE constraints with a relative tolerance of 1×10^{-5} were used on all hydrogen-heavy atom bonds to permit a dynamics time step of 2 fs. Electrostatic interactions were calculated by the particle mesh Ewald method (PME) (*32*). The Lennard-Jones cutoffs were set at 1.0 nm. The rmsd of each simulated system was calculated over the MD simulations to make sure that the system reached equilibration.

Conformational and Structural Analyses. With the MD simulation trajectories after equilibration, we performed conformational analysis, secondary structure analysis, and hydrogen bond analysis to understand the molecular and structural basis for the critical role of TSP1 residues 24 and 32 and CRT residues 24−26 and 32−34 in TSP1−CRT binding. We calculated the root-mean-square fluctuations (rmsfs) of the wild-type TSP1 N-domain (TSP1), the TSP1 K24A/K32A mutant, wild-type CRT, and the CRT mutant with mutations of residues 24−26 and 32−34 to Ala. In addition to rmsf analyses, we also analyzed the dynamical cross-correlation map among the residues of TSP1, CRT, and their mutants. Through these analyses, we investigated the changes in the conformational flexibility and the degree of correlated motion between residues in the protein by the mutation of the key residues. We calculated the changes in hydrogen bond formation in the β-sheet region and the changes of the residues of β-strand occupancy for the TSP1 N-domain and CRT to evaluate structural changes of the protein by mutation of the key residues. A hydrogen bond was assigned when the distance between the hydrogen and acceptor was less than 4 Å, and the donor−hydrogen−acceptor angle is less than 30°. OH and NH groups were treated as donors; oxygen or nitrogen was defined as the acceptor. The occupancy of each hydrogen bond was calculated on the basis of the percentage of time that the hydrogen bond existed over the entire simulation time. The hydrogen bond occupancy of each β-strand pair in the TSP1 N-domain and CRT was considered to be the average occupancy of the hydrogen bonds of each β-strand pair. A β-strand is typically 3−10 amino acids long with its backbone in an almost fully extended conformation; however, β-strands are rarely perfectly extended. If the dihedral angles (φ and ψ) of an amino acid with its adjacent residues were near −135° and 135°, respectively, the amino acid was assigned to be contained in the β-strand. The occupancy of each residue in the β-strand was determined on the basis of the percentage of time that the residue existed in the β-strand over the simulation.

RESULTS AND DISCUSSION

Effect of the Mutations of the Key Residues in TSP1 and CRT on TSP1−CRT Binding from SMD Simulation. We first validated the SMD simulation results with respect to the effect of the mutations of the key residues in TSP1 and CRT on TSP1−CRT binding via experimental observation (*3*, *4*, *7*). Under constant-velocity SMD simulations, it was shown that around 60 ps, the buried protein surface area (BPSA) for the TSP1−CRT complex was decreased from 2142 to 1482 Å^2, the BPSA of the TSP1 K24A/K32A mutant−CRT complex from 2182 to 1279 Å^2, and the BPSA of the TSP1−CRT mutant complex with residues 24−26 and 32−34 of CRT mutated to Ala from 2160 to 1087 Å^2 (Figure 2A). The significantly decreased BPSA indicated the reduced level of binding of TSP1 and CRT. The force required to break the binding of the wild-type TSP1−CRT complex

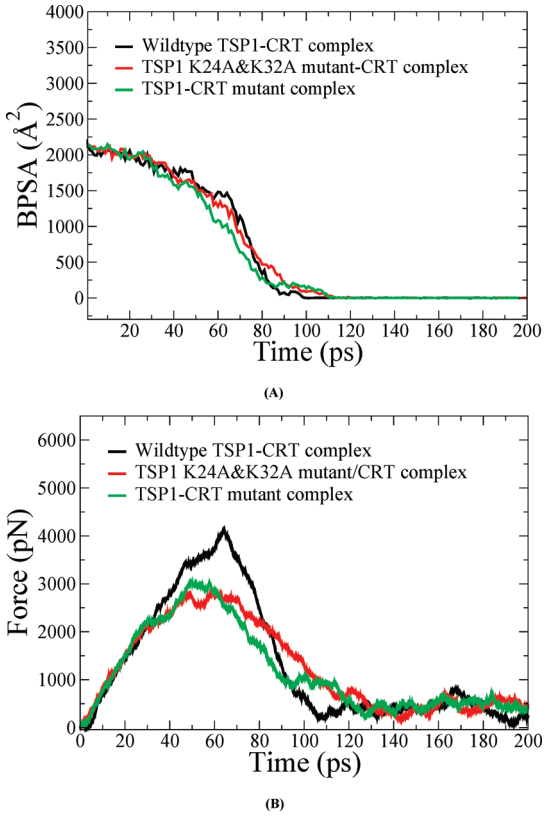

FIGURE 2: (A) Buried protein surface area (BPSA) for the TSP1−CRT complex, the TSP1 K24A/K32A mutant−CRT complex, and the TSP1−CRT mutant complex over the course of constant-velocity SMD simulation. (B) Force experienced in the TSP1−CRT complex, the TSP1 K24A/K32A mutant−CRT complex, and the TSP1−CRT mutant complex over the course of constant-velocity SMD simulation.

(~4000 pN) was much larger than that of the TSP1 mutant−CRT complex and of the TSP1−CRT mutant complex (~3000 pN) (Figure 2B). These calculated results showed that mutation of residues 24 and 32 to Ala in TSP1 and of amino acids 24−26 and 32−34 to Ala in CRT resulted in a decreased level of binding between TSP1 and CRT. TSP1 K24A and K32A mutations and mutations of amino acids 24−26 and 32−34 to Ala in CRT directly affect the electrostatic interactions between TSP1 and CRT as observed in our previous thermodynamics study of the TSP1−CRT complex (*20*). In addition to the effect on electrostatic interactions between TSP1 and CRT, TSP1 K24A and K32A mutations and mutations of amino acids 24−26 and 32−34 to Ala in CRT caused significant changes in the van der Waals energy, polar solvation energy, and entropy of the TSP1−CRT complex and, thereby, significantly decreased the binding free energy of the TSP1−CRT complex (*20*). Experimental studies also showed that a peptide with mutations of residues 24 and 32 to Ala does not signal focal adhesion disassembly or stimulate collagen (*9*). Simple electrostatic interactions are not the sole determinant of binding because a scrambled CRT binding sequence peptide (scrambled hep I) does not signal focal adhesion disassembly or block TSP1 stimulation of collagen (*9*, *16*). Our previous binding thermodynamic results (*20*) help in the interpretation of the results from the SMD simulations that TSP1 K24A and K32A mutations and mutations of amino acids 24−26 and 32−34 to Ala in CRT decreased the resistance to force-induced dissociation of the TSP1−CRT complex. Biochemical binding studies (immunoprecipitation) have been used to show that purified TSP1 and CRT bind to each other and that complex formation can be disrupted by the hep I peptide, but not by the hep I peptide with residues 24 and 32 mutated to Ala (*3*). Furthermore, CRT null cells engineered to express CRT lacking the TSP1 binding site were refractory to TSP1-induced signaling of resistance to anoikis, and a peptide of the TSP binding sequence of CRT, but not the mutated binding sequence, blocks TSP1 stimulation of collagen expression (*4*, *7*, *9*). The calculated results obtained from these studies are thus consistent with the results of previous biochemical and cell-based studies of the role of these sequences in mediating TSP1−CRT binding and signaling (*3*, *4*, *7*). Moreover, the CRT mutations could also affect binding of CRT to LRP1, thereby disrupting the formation of the TSP1−CRT−LRP1 ternary complex for signaling the cellular activities (*6*).

In the constant-force SMD simulations, the extension profile for the TSP1−CRT complex, the TSP1 K24A/K32A mutant−CRT complex, and the TSP1−CRT mutant complex showed that under the same external load pulling, it took more time to significantly increase the distance between the centers of mass of the binding sites of the TSP1−CRT complex for the wild-type TSP1−CRT complex than for its mutants (Figure 2S of the Supporting Information). The structure of the TSP1−CRT complex with the binding sites of the TSP1−CRT complex highlighted is shown in Figure 1S of the Supporting Information. During the calculated disruption of the TSP1−CRT complex(s) under external load pulling, the relative rotational motion between TSP1 and CRT could increase, and therefore, it is not surprising that the distance between the centers of mass of the binding sites of the TSP1 K24A/K32A mutant−CRT complex decreased before unbinding as observed in Figure 2S of the Supporting Information. The results showed that TSP1 K24A and K32A mutations and mutations of amino acids 24−26 and 32−34 to Ala in CRT significantly decreased the strength of binding between TSP1 and CRT, consistent with the biochemical and cell biological experimental results (*3*, *4*, *7*).

Conformational and Structural Changes in TSP1 Caused by the Mutations of Residues 24 and 32 to Ala. (*i*) *Conformational Changes in TSP1*. The rmsd of TSP1 and the K24A/K32A mutant over the 30 ns MD simulations exhibited initial equilibration after 10 ns MD simulations (Figure 3S of the Supporting Information). The simulation trajectories from 10 to 30 ns were used for conformational and structural analyses. The crystal structure of the TSP1 N-domain shows that the TSP1 binding site for CRT spans the α1 helix to the β2 strand, which is a flexible and exposed loop region with a short β-strand as shown in Figure 1S of the Supporting Information (*17*). For the wild-type TSP1 N-domain and the TSP1 K24A/K32A mutant, the rmsf, calculated by averaging MD trajectories from 10 to 30 ns, showed that TSP1 K24A and K32A mutations resulted in the changes in TSP1 conformational flexibility, including an increased conformational fluctuation of the TSP1 binding site for CRT and the decreased fluctuation for residues 94, 95, 108, 120, and 161−163 (Figure 3A). The increased fluctuation of the TSP1 binding site for CRT and the changed fluctuation of other residues could directly affect the electrostatic interactions and van der Waals interactions between TSP1 and CRT as observed in our previous thermodynamics study (*20*), including the prevention of forming specific side chain interactions at the binding sites. These changes could contribute to the loss of binding between TSP1 and CRT as observed in biochemical experiments (*3*, *16*). The changed conformational fluctuation of TSP1 in the regions other than binding site of CRT in TSP1 could also affect binding to other ligands for the TSP1 N-domain such as integrins.

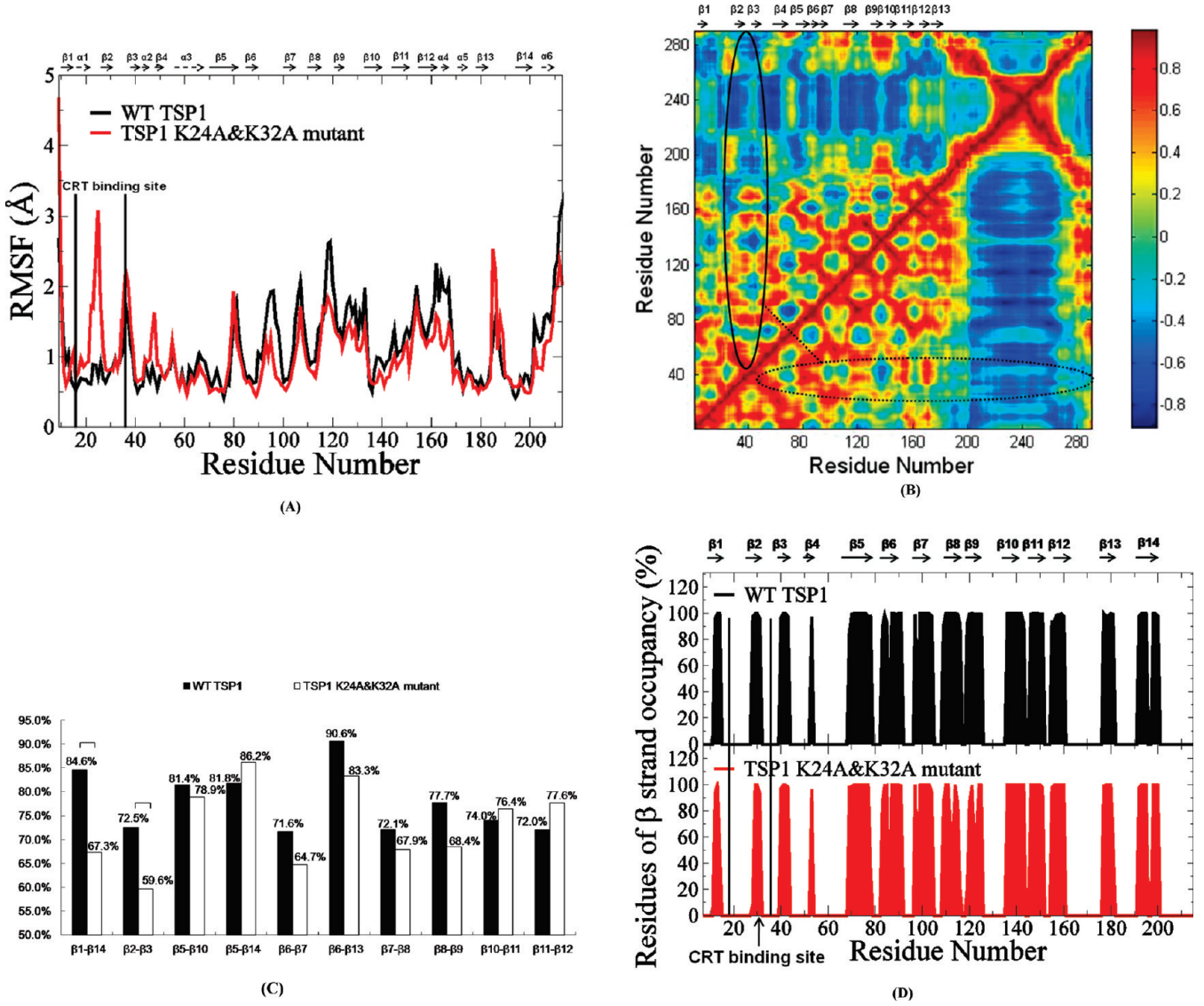

FIGURE 3: (A) Root-mean squared fluctuations (rmsf) of the TSP1 N-domain. β-Strands and α-helices corresponding to the residues in TSP1 are marked atop panel A. (B) Dynamical cross-correlation map for the degree of correlated motion of the residues in TSP1 (red for correlated motion between residues, blue for anticorrelated motion between residues, and circled region for the correlated motion between the residues in the binding site of TSP1 for CRT and the other residues of TSP1). Wild-type TSP1 (top left) compared to the TSP1 K24A/K32A mutant (bottom right). β-Strands and α-helices corresponding to the residues in TSP1 are marked atop the dynamical cross-correlation map. (C) Hydrogen bond occupancy of each β-strand pair in TSP1. (D) Residues of β-strand occupancy in TSP1.

The dynamical cross-correlation maps for TSP1 and its mutant are shown in Figure 3B, in which wild-type TSP1 is represented in the top left half and the TSP1 K24A/K32A mutant in the bottom right half. Dynamical cross-correlation mapping showed that K24A and K32A mutations in TSP1 resulted in an overall decreased degree of correlated motion between the residues in TSP1, evidenced by fewer red patches (correlated motions) and blue patches (anticorrelated motions) compared to those for wild-type TSP1. Results also showed that the degree of correlated motion between the residues in the TSP1 binding site for CRT and the other residues in CRT was reduced by the K24A and K32A mutations in TSP1 (circled in Figure 3B). Our previous study of the binding thermodynamics of the TSP1−CRT complex showed that the TSP1 K24A and K32A mutations significantly decreased the binding free energy of the TSP1−CRT complex, including the significant changes in the electrostatic energy, van der Waals energy, polar solvation energy, and entropy of the TSP1−CRT complex (*20*). These changes in the degree of correlated motion for the residues in TSP1 and in the conformational flexibility of TSP1 by TSP1 K24A and K32A mutations could directly cause the changes in the electrostatic energy, van der Waals energy, polar solvation energy, and entropy for interactions of TSP1 with CRT and, thereby, contribute to loss of TSP1 and CRT binding.

(*ii*) *Changes in Hydrogen Bond and β-Strand Formation in TSP1*. The globular TSP1 N-domain is primarily composed of 13 antiparallel β-strands, one irregular strandlike segment, and six α-helices that are located either between β-strands or in the C-terminal area (*17*). The hydrogen bonds formed between β-strands play an important role in protein structural stability. Analysis of the formation of hydrogen bonds between β-strands and their occupancy over the last 20 ns of MD simulation trajectories showed that the TSP1 K24A and K32A mutations resulted in a >10% decrease in hydrogen bond occupancy between strands β1 and β14 and strands β2 and β3 when compared to that of the wild-type TSP1 N-domain (Figure 3C). Structures of the wild-type TSP1 N-domain and the TSP1 N-domain K24A/K32A mutant are shown in Figures 5S and 6S of the Supporting

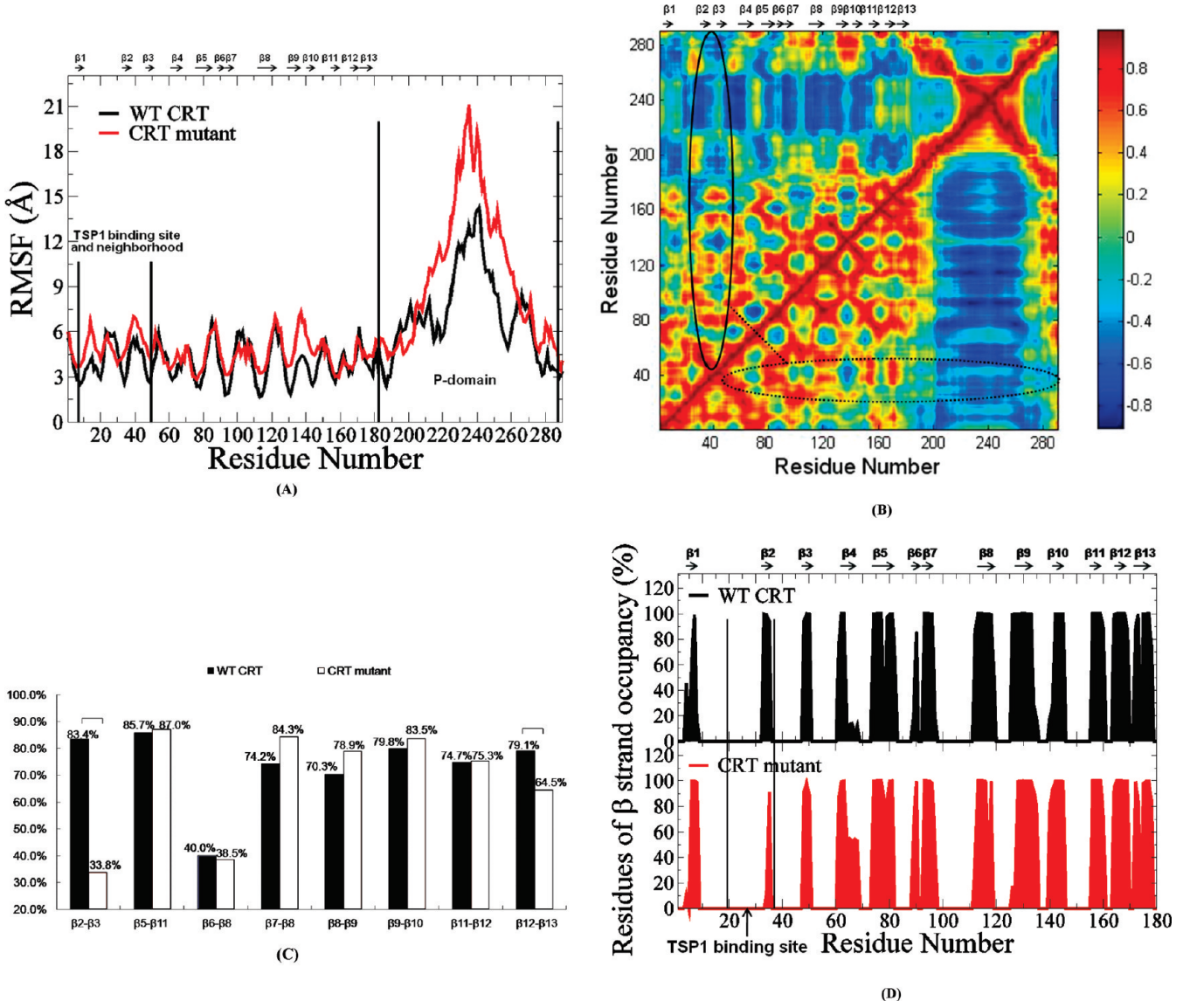

FIGURE 4: (A) rmsf of CRT. β-Strands corresponding to the residues in CRT are marked atop panel A. (B) Dynamical cross-correlation map for the degree of correlated motion of the residues in CRT (red for correlated motion, blue for anticorrelated motion, and circled region for correlated motion between the residues in the binding site of CRT for TSP1 and other residues of CRT). Wild-type CRT (top left) compared to CRT mutant (residues 24−26 and 32−34 mutated to Ala) (bottom right). β-Strands corresponding to the residues in CRT are marked atop the dynamical cross-correlation map. (C) Hydrogen bond occupancy of each β-strand pair in CRT. (D) Residues of β-strand occupancy in CRT.

Information for comparison of β1−14 and β2−3 strands of the wild-type and mutant TSP1. Strand β2 is located within the region of residues 17−35 that is found in the TSP1 binding site for CRT, and strand β3 is adjacent to strand β2 (*17*). Strand β1 is connected to strand β2 through helix α1, and strand β14 is adjacent to strand β1 (*17*). The significantly decreased hydrogen bond occupancy between strands β2 and β3 and between strands β1 and β14 caused by TSP1 K24A and K32A mutations (Figure 3C and Table 1S of the Supporting Information) could affect the conformational stability of the TSP1 binding site for CRT and the overall conformational stability of TSP1.

Analyses of β-strand formation over the last 20 ns MD simulation trajectories showed that TSP1 K24A and K32A mutations resulted in the shortened β2 strand (Figure 3D). The residues in strand β2 included amino acids R28, R29, L30, and V31. The occupancies of the four residues in strand β2 were 98, 100, 100, and 96% for wild-type TSP1 and 9, 100, 100, and 93% for the TSP1 K24A/K32A mutant, respectively. Amino acid R28 was rarely in strand β2 with TSP1 K24A and K32A mutations, resulting in the shortened β2 strand. The shortened β2 strand could contribute to the decrease in hydrogen bond occupancy between β2 and β3 by TSP1 K24A and K32A mutations as observed in Figure 3C and Table 1S of the Supporting Information. The hydrogen bond and β-strand formation changed by TSP1 K24A and K32A mutations could contribute to the changes in TSP1 conformation as observed in rmsf and dynamical cross-correlation analyses and also provide the structural and molecular basis of the observed loss of protein binding and cell function upon mutation of Lys 24 and Lys 32 of TSP1 to Ala (*3*, *16*).

Conformational and Structural Changes in CRT Caused by the Mutations of Amino Acids 24−26 and 32−34 to Ala. (*i*) *Conformational Changes in CRT.* The rmsd of CRT and the CRT mutant over the 30 ns MD simulations showed that the system reached initial equilibration after 10 ns MD simulations (Figure 4S of the Supporting Information). The TSP1 binding site in CRT has been localized to the sequence of residues 19−36 in the N-domain of CRT (*4*), and CRT with residues 24−26 and 32−34 mutated to Ala is unable to mediate

anoikis resistance or focal adhesion disassembly upon stimulation with TSP1 (*7*). The structure of CRT showed that the CRT binding site for TSP1 covers regions of strand β2 in CRT (*19*). The rmsf calculated over the last 20 ns MD simulation trajectories for both wild-type CRT and the CRT mutant showed that the mutations of CRT residues 24−26 and 32−34 to Ala resulted in increased conformational fluctuation of the CRT binding site for TSP1 and its adjacent regions and resulted in increased conformational fluctuation of the middle region of the CRT P-domain (Figure 4A), which could affect binding of CRT to TSP1 as that observed in the experiments (*7*). The dynamical cross-correlation maps for CRT and its mutant are shown in Figure 4B, in which the top left half represents wild-type CRT and the bottom right half the CRT mutant. Results showed that mutations of CRT residues 24−26 and 32−34 to Ala resulted in an increased correlated movement (red) within the N-domain of CRT [residues (res) 1−180] and an increased anticorrelated motion (blue) between the N-domain of CRT (res 1−180) and the P-domain of CRT (res 181−290) as compared to those for wild-type CRT. The changed degree of correlated motion by the mutations of residues 24−26 and 32−34 to Ala was also observed for the CRT binding site for TSP1 relative to the other residues of CRT (circled in Figure 4B). These changes in the degree of correlated motion for the residues in CRT and in the conformational flexibility of the CRT−TSP1 complex caused by the mutations of residues 24−26 and 32−34 to Ala could directly result in the changes in the electrostatic energy, van der Waals energy, polar solvation energy, and entropy for interactions of CRT with TSP1, affecting TSP1−CRT binding as observed in our previous thermodynamics study (*20*) and in cell-based experiments (*7*).

(*ii*) *Changes in Hydrogen Bond and* β*-Strand Formation in CRT*. The CRT structural model shows that CRT is mainly composed of a structurally stable globular N-domain formed by antiparallel β-sheets and a flexible P-domain with an extended arm structure (*19*). The CRT binding site for TSP1 (res 19−36) is located within the CRT N-domain and spans strand β2 (*4*, *19*). We analyzed the hydrogen bonds and their occupancy between β-strands over the last 20 ns MD simulations for wild-type CRT and the CRT mutant (res 24−26 and 32−34 mutated to Ala). Almost 50% decreased hydrogen bond occupancy between strands β2 and β3 and more than 10% decreased hydrogen bond occupancy between strands β12 and β13 resulted from the mutations of CRT res 24−26 and 32−34 to Ala (Figure 4C and Table 2S of the Supporting Information).

Analyses of β-strand formation over the last 20 ns MD simulation trajectories showed that mutations of CRT residues 24−26 and 32−34 to Ala resulted in the shortened β2 strand (Figure 4D). The residues in strand β2 included amino acids V33, L34, and S35. The occupancies of the three residues in strand β2 were 100, 99, and 95% for wild-type CRT and 0, 13, and 91% for the CRT mutant, respectively. Amino acids V33 and L34 were rarely in strand β2 after the mutations of CRT res 24−26 and 32−34 to Ala, causing the shortened β2 strand. The shortened β2 strand could contribute to the decreased hydrogen bond occupancy between strands β2 and β3 caused by mutations of residues 24−26 and 32−34 to Ala in CRT as observed in Figure 4C and Table 2S of the Supporting Information. Strand β2 (res 33−35) is located within the CRT binding site for TSP1, and strands β12 and β13 are located near the CRT binding site for TSP1 (*19*). The changed β2 strand and significantly decreased hydrogen bond occupancy between strands β2 and β3 and between strands β12 and β13 caused by the mutations of CRT residues 24−26 and 32−34 to Ala could change the conformational stability of the CRT binding site for TSP1 and the overall conformational stability of CRT as observed in rmsf and dynamical cross-correlation analyses, which could weaken the binding of TSP1 to CRT. These results provide a molecular and structural basis for the experimental observation that the mutations of CRT res 24−26 and 32−34 to Ala weaken TSP1−CRT binding and weaken the signaling of anoikis resistance (*7*).

CONCLUSIONS

In this study, we used simulation results examining the effect of mutation of key residues in TSP1 and CRT on TSP1−CRT binding to validate experimental biochemical observations. Using MD simulations, we elucidated the molecular and structural basis for the critical role of residues 24 and 32 in TSP1 and residues 24−26 and 32−34 in CRT for TSP1−CRT binding as observed in biochemical studies. Mutations of residues 24 and 32 to Ala in TSP1 and mutations of residues 24−26 and 32−34 to Ala in CRT resulted in an increased conformational flexibility of the binding site and an overall changed conformational flexibility of the protein, a changed degree of dynamical correlated motion between the residues in the binding site and other residues in the protein, and a changed degree of overall correlated motions between the residues in the protein. Mutation of the key residues in TSP1 and CRT also caused shortening of the β-strand in the binding site and decreased hydrogen bond occupancy for β-strand pairs within or near its binding site for the other protein. These changes could directly result in alterations in the electrostatic energy, van der Waals energy, polar solvation energy, and entropy for interactions of TSP1 with CRT, contributing to the loss of or weakened binding of the TSP1−CRT complex with resultant attenuation of TSP1−CRT binding-induced cellular activities. These studies provide new knowledge regarding the structural basis of these interactions with the potential for developing drug candidates and other strategies for the allosteric regulation of TSP1−CRT binding and its induced cellular activities.

ACKNOWLEDGMENT

We acknowledge Dr. Marek Michalak for providing the PDB file of calreticulin. We thank the anonymous reviewers for their helpful remarks.

SUPPORTING INFORMATION AVAILABLE

Constructed TSP1−CRT complex from our previous study (Figure 1S); simulation protocol and the results of constant-force SMD for the TSP1−CRT complex, the TSP1 K24A/K32A mutant−CRT complex, and the TSP1−CRT mutant complex (Figure 2S); rmsd of TSP1 and its mutant and rmsd of CRT and its mutant over the MD simulations showing that that the system reached the initial equilibration after MD simulation for 10 ns (Figures 3S and 4S, respectively); structures of the wild-type TSP1 N-domain and TSP1 N-domain K24A/K32A mutant for comparison of the strands β1 and β14 and strands β2 and β3 of the wild-type and mutant TSP1 (Figures 5S and 6S, respectively); occupancy of the hydrogen bond formed between residues in the β-strands of TSP1 and its mutant over the last 20 ns MD simulation trajectories (Table 1S); and occupancy of the hydrogen bond formed between residues in the β-strands of CRT and its mutant over the last 20 ns MD simulation trajectories

(Table 2S). This material is available free of charge via the Internet at http://pubs.acs.org.

REFERENCES

1. Murphy-Ullrich, J. E. (2001) The de-adhesive activity of matricellular proteins: Is intermediate cell adhesion an adaptive state? *J. Clin. Invest. 107*, 785–790.
2. Greenwood, J. A., and Murphy-Ullrich, J. E. (1998) Signaling of de-adhesion in cellular regulation and motility. *Microsc. Res. Tech. 43*, 420–432.
3. Goicoechea, S., Orr, A. W., Pallero, M. A., Eggleton, P., and Murphy-Ullrich, J. E. (2000) Thrombospondin mediates focal adhesion disassembly through interactions with cell surface calreticulin. *J. Biol. Chem. 275*, 36358–36368.
4. Goicoechea, S., Pallero, M. A., Eggleton, P., Michalak, M., and Murphy-Ullrich, J. E. (2002) The anti-adhesive activity of thrombospondin is mediated by the N-terminal domain of cell surface calreticulin. *J. Biol. Chem. 277*, 37219–37228.
5. Orr, A. W., Elzie, C. A., Kucik, D. F., and Murphy-Ullrich, J. E. (2003) Thrombospondin signaling through the calreticulin/LDL receptor-related protein co-complex stimulates random and directed cell migration. *J. Cell Sci. 116*, 2917–2927.
6. Orr, A. W., Pedraza, C. E., Pallero, M. A., Elzie, C. A., Goicoechea, S., Strickland, D. K., and Murphy-Ullrich, J. E. (2003) Low density lipoprotein receptor-related protein is a calreticulin coreceptor that signals focal adhesion disassembly. *J. Cell Biol. 161*, 1179–1189.
7. Pallero, M. A., Elzie, C. A., Chen, J., Mosher, D. F., and Murphy-Ullrich, J. E. (2008) Thrombospondin 1 binding to calreticulin-LRP1 signals resistance to anoikis. *FASEB J. 22*, 3968–3979.
8. Elzie, C. A., and Murphy-Ullrich, J. E. (2004) The N-terminus of thrombospondin: The domain stands apart. *Int. J. Biochem. Cell Biol. 36*, 1090–1101.
9. Sweetwyne, M. T., Pallero, M. A., Lu, A., Van Duyn Graham, L., and Murphy-Ullrich, J. E. (2010) The calreticulin-binding sequence of thrombospondin 1 regulates collagen expression and organization during tissue remodeling. *Am. J. Pathol. 177*, 1710–1724.
10. Bornstein, P. (2001) Thrombospondins as matricellular modulators of cell function. *J. Clin. Invest. 107*, 929–934.
11. Bornstein, P. (1995) Diversity of function is inherent in matricellular proteins: An appraisal of thrombospondin 1. *J. Cell Biol. 130*, 503–506.
12. Carlson, C. B., Bernstein, D. A., Annis, D. S., Misenheimer, T. M., Hannah, B. L., Mosher, D. F., and Keck, J. L. (2005) Structure of the calcium-rich signature domain of human thrombospondin-2. *Nat. Struct. Mol. Biol. 12*, 910–914.
13. Norgaard Toft, K., Larsen, N., Steen Jorgensen, F., Hojrup, P., Houen, G., and Vestergaard, B. (2008) Small angle X-ray scattering study of calreticulin reveals conformational plasticity. *Biochim. Biophys. Acta 1784*, 1265–1270.
14. Ellgaard, L., Riek, R., Braun, D., Herrmann, T., Helenius, A., and Wuthrich, K. (2001) Three-dimensional structure topology of the calreticulin P-domain based on NMR assignment. *FEBS Lett. 488*, 69–73.
15. Tan, Y., Chen, M., Li, Z., Mabuchi, K., and Bouvier, M. (2006) The calcium- and zinc-responsive regions of calreticulin reside strictly in the N-/C-domain. *Biochim. Biophys. Acta 1760*, 745–753.
16. Murphy-Ullrich, J. E., Gurusiddappa, S., Frazier, W. A., and Hook, M. (1993) Heparin-binding peptides from thrombospondins 1 and 2 contain focal adhesion-labilizing activity. *J. Biol. Chem. 268*, 26784–26789.
17. Tan, K., Duquette, M., Liu, J. H., Zhang, R., Joachimiak, A., Wang, J. H., and Lawler, J. (2006) The structures of the thrombospondin-1 N-terminal domain and its complex with a synthetic pentameric heparin. *Structure 14*, 33–42.
18. Schrag, J. D., Bergeron, J. J., Li, Y., Borisova, S., Hahn, M., Thomas, D. Y., and Cygler, M. (2001) The Structure of calnexin, an ER chaperone involved in quality control of protein folding. *Mol. Cell 8*, 633–644.
19. Guo, L., Groenendyk, J., Papp, S., Dabrowska, M., Knoblach, B., Kay, C., Parker, J. M., Opas, M., and Michalak, M. (2003) Identification of an N-domain histidine essential for chaperone function in calreticulin. *J. Biol. Chem. 278*, 50645–50653.
20. Yan, Q., Murphy-Ullrich, J. E., and Song, Y. (2010) Structural insight into the role of thrombospondin-1 binding to calreticulin in calreticulin-induced focal adhesion disassembly. *Biochemistry 49*, 3685–3694.
21. Phillips, J. C., Braun, R., Wang, W., Gumbart, J., Tajkhorshid, E., Villa, E., Chipot, C., Skeel, R. D., Kale, L., and Schulten, K. (2005) Scalable molecular dynamics with NAMD. *J. Comput. Chem. 26*, 1781–1802.
22. Jorgensen, W. L., Chandrasekhar, J., Madura, J. D., Impey, R. W., and Klein, M. L. (1983) Comparison of simple potential functions for simulating liquid water. *J. Chem. Phys. 79*, 926–935.
23. Pan, D., and Song, Y. (2010) Role of Altered Sialylation of the I-like Domain of β1 Integrin in the Binding of Fibronectin to β1 Integrin: Thermodynamics and Conformational Analyses. *Biophys. J. 99*, 208–217.
24. Suever, J. D., Chen, Y., McDonald, J. M., and Song, Y. (2008) Conformation and free energy analyses of the complex of calcium-bound calmodulin and the Fas death domain. *Biophys. J. 95*, 5913–5921.
25. Liu, Y., Pan, D., Bellis, S. L., and Song, Y. (2008) Effect of altered glycosylation on the structure of the I-like domain of β1 integrin: A molecular dynamics study. *Proteins 73*, 989–1000.
26. Song, Y., Guallar, V., and Baker, N. A. (2005) Molecular dynamics simulations of salicylate effects on the micro- and mesoscopic properties of a dipalmitoylphosphatidylcholine bilayer. *Biochemistry 44*, 13425–13438.
27. Izrailev, S., Stepaniants, S., Balsera, M., Oono, Y., and Schulten, K. (1997) Molecular dynamics study of unbinding of the avidin-biotin complex. *Biophys. J. 72*, 1568–1581.
28. Lu, H., Isralewitz, B., Krammer, A., Vogel, V., and Schulten, K. (1998) Unfolding of titin immunoglobulin domains by steered molecular dynamics simulation. *Biophys. J. 75*, 662–671.
29. Gao, M., Craig, D., Vogel, V., and Schulten, K. (2002) Identifying unfolding intermediates of FN-III(10) by steered molecular dynamics. *J. Mol. Biol. 323*, 939–950.
30. Hytonen, V. P., and Vogel, V. (2008) How force might activate talin's vinculin binding sites: SMD reveals a structural mechanism. *PLoS Comput. Biol. 4*, No. e24.
31. Case, D. A., Cheatham, T. E., III, Darden, T., Gohlke, H., Luo, R., Merz, K. M., Jr., Onufriev, A., Simmerling, C., Wang, B., and Woods, R. J. (2005) The Amber biomolecular simulation programs. *J. Comput. Chem. 26*, 1668–1688.
32. Darden, T., York, D., and Pedersen, L. G. (1993) Particle mesh Ewald: An N.log(N) method for Ewald sums in large systems. *J. Chem. Phys. 98*, 10089–10092.